Journal of Solid State Chemistry 193 (2012) 147–153

Contents lists available at SciVerse ScienceDirect

Journal of Solid State Chemistry

journal homepage: www.elsevier.com/locate/jssc

N-type thermoelectric recycled carbon fibre sheet with electrochemically deposited Bi_2Te_3

E.J.X. Pang [a], S.J. Pickering [a,*], A. Chan [b], K.H. Wong [a], P.L. Lau [b]

[a] Division of Materials, Mechanics and Structures, The University of Nottingham, University Park, Nottingham, NG7 2RD, UK
[b] Division of Materials, Mechanics and Structures, The University of Nottingham Malaysia Campus, Jalan Broga, 43500 Semenyih, Selangor Darul Ehsan, Malaysia

ARTICLE INFO

Article history:
Received 21 November 2011
Received in revised form
3 April 2012
Accepted 29 April 2012
Available online 12 May 2012

Keywords:
Recycled carbon fibres
Seebeck coefficient
Electrical resistivity
Bismuth telluride

ABSTRACT

An N-type thermoelectric recycled carbon fibre sheet with bismuth telluride coating has been successfully synthesised through an electro-deposition technique. The Seebeck coefficient and electrical properties of the combined recycled carbon fibre sheet and bismuth telluride films are reported. Classification of the crystal structure, surface morphology and the elemental composition of the resulting deposits are methodically characterised by XRD, SEM and EDX. Cyclic voltammetry is also carried out in nitric acid solutions to investigate the right range of deposition potential. The synthesis N-type thermoelectric sheet has a highest attainable Seebeck coefficient of $-54\,\mu V\,K^{-1}$ and an electrical resistivity of $8.9\times10^{-5}\,\Omega\,m$. The results show slight differences in morphologies and thermoelectric properties for the films deposited at varying deposition potential. The increase in thermoelectrical properties of the recycled carbon fibre is in line with the development of using coated recycled fibre for thermoelectrical applications.

1. Introduction

Since the advent of carbon fibres in the late 20th century, carbon fibres have found increasing usage in the aerospace and sport goods industries. The rising increase in composite usage has caused an end-of-life concern. With the current Landfill Directive (1999/31/EC) by the European Union applied in 1999, it has effectively restricted composite waste to be disposed of as a chemical waste. Hence recycling composites and reclamation of fibres would not only save disposal cost, but give an outlet for the fibres to be reused for existing and new applications.

The recycling of carbon fibre composites poses a challenge where a thermosetting resin matrix is used, causing it to be irreversible once cross-linked. With recent developments, carbon fibre composites can now be recycled through various methods such as fluidised bed [1,2], pyrolysis [3] and the use of super-critical fluids [4,5]. Many current routes to reuse the recycled carbon fibres mainly focus on its mechanical properties while recycled carbon fibres are also found to be a suitable candidate as an electromagnetic interference shielding material [6]. In order to ensure a close recycling loop, ways to reuse the recycled fibres need to be explored.

Not much attention has been paid to carbon fibre's electrical properties, in fact carbon fibre has low electrical resistivity and is easy to tamper with its Seebeck coefficient [7–11]. This paves the way to utilise recycled carbon fibres in combination with thermoelectric coatings as a flexible thermoelectric material.

In order to achieve an optimal performance for thermoelectric applications, an efficient thermoelectric material is required. The quality performance of a thermoelectric material can be measured through a parameter called the figure of merit [11]

$$z_T = T\alpha^2/\rho k \quad (1)$$

where ρ is the electrical resistivity; k is the thermal conductivity; T is the temperature and α is the Seebeck coefficient of the material. Bismuth telluride, Bi_2Te_3 is well known to possess a very high figure of merit at room temperature. Hence it is one of the most used thermoelectric materials in the market. Various methods such as sputtering [12], chemical vapour deposition (CVD) [13], evaporation [14,15] and electro-depostion [16–18] techniques have been developed for the synthesis of bismuth telluride thin films. The latter however tends to provide a cost-effective alternative and it is also relatively easy to control. Bismuth telluride has been successfully synthesised using present electro-deposition techniques by Kobayashi [19] and achieved a maximum Seebeck coefficient of around $250\,\mu V\,K^{-1}$.

Many researchers have also used a nitric acid–based bath with metal substrates such as nickel, silver, platinum and titanium [20] for synthesis. However none have reported the thermoelectrical properties for the combination of both the thin film and substrate. In this particular case, recycled carbon fibre was used as a working electrode/substrate as it is naturally conductive, strong and

* Corresponding author. Fax: +44 0115 951 3800.
E-mail address: stephen.pickering@nottingham.ac.uk (S.J. Pickering).

0022-4596
http://dx.doi.org/10.1016/j.jssc.2012.04.046

flexible. These attributes suggest that compliant recycled carbon fibre sheets can be reused with minimal parasitic additions while preserving its own good properties and improving its thermoelectrical properties with the combination of the thermoelectric film. This is in line with the development of a flexible cooling fabric where the combination of both the recycled carbon fibre and bismuth telluride would yield an efficient yet flexible thermoelectric material.

The use of electro-deposition is also ideal as the creation of P and N-type materials could be easily tailored by controlling the deposition potential. The P and N-type semiconductor nature of bismuth telluride relies heavily on the composition where a bismuth rich type usually yields a P-type material while a tellurium rich compound yields an N-type material [21]. The present work focuses on synthesising a novel and efficient thermoelectric material using recycled carbon fibre as a substrate while paying attention to the electrochemical synthesising process of Bi_2Te_3 on the recycled carbon fibre. The classification of the crystal structure, surface morphology and the elemental composition of the resulting deposits are methodically characterised by X-ray diffraction (XRD), Scanning electron microscope (SEM) and energy dispersive X-ray (EDX) correspondingly.

2. Methodology

2.1. Materials

The carbon fibre used in the experiments is in the form of T-800s PAN-based recycled carbon fibre provided by the Recycled Carbon Fibre Limited (RCF) Coseley, UK. The fibre had a diameter of 5 μm, specific density of 1.8, tensile strength and Young modulus of 5.88 GPa and 294 GPa respectively [22]. The fibre was recycled from a toughened epoxy composite scrap through a pyrolysis process. The recycled carbon fibre was then manufactured into a sheet using a standard wet papermaking method.

2.2. Electrochemical experiments

Bi_2Te_3 films were electrodeposited on a recycled carbon fibre sheet from an aqueous nitric acid bath containing 8 mM of Bi^{3+} and 10 mM of $HTeO_2^+$. The ions were formed using bismuth (III) nitrate pentahydrate, $BiN_3O_9 \cdot 5H_2O$ and tellurium oxide, TeO_2, both of them were obtained from Sigma Aldrich. All the electrochemical experiments were conducted using a potentiotstat (VersaStat-3, Princeton Applied Research) at room temperature. A standard 3-cell electrode configuration was used with the combination of a potentiostat in order to accurately control the deposition voltage. The reference electrode was a silver/silver chloride filled with 1 M of KCl and the counter electrode is a platinum rod. Fig. 1 shows the schematic of the experimental setup. The working electrode consists of a recycled carbon fibre sheet with a dimension of 1.5 cm by 3 cm. Constant agitation was provided during the uniform voltage deposition stage onto the substrate. Cyclic voltammograms were also performed in an unstirred solution using the similar potentiostat at a scan rate of 10 mV s^{-1}.

2.3. Seebeck coefficient measurements

The Seebeck coefficient or thermopower, α is an intrinsic property of a material which is related to the material's electronic structure, and independent of its geometry [23]. The Seebeck coefficient of the recycled carbon fibre sheet was measured through Eq. (2). This method requires the pre-requisite knowledge of the reference material's absolute thermoelectric power due to its relative measurements,

$$\alpha_{AB} = \frac{\Delta V}{\Delta T} = \frac{(V_H - V_L)}{(T_H - T_L)} \quad (2)$$

where $\alpha_{AB} = \alpha_b - \alpha_A$ is the measured value which includes the sample contribution α_A and the reference contribution α_b [23]. Therefore the absolute Seebeck coefficient of the sample can becomputed as $\alpha_A = \alpha_b - \alpha_{AB}$. It is easy to get a mistaken sign of ($\pm$) of the absolute Seebeck coefficient values where usually the sample's Seebeck coefficient is the opposite sign of the measured value [24]. Appropriate care must be exercised when conducting and interpreting the measurements.

The measurements of the Bi_2Te_3 coated recycled T-800s carbon fibre sheet's Seebeck coefficient were conducted by applying a conducting silver epoxy adhesive on the two ends of the sheet onto the copper foil. A copper wire is then soldered to each ends of the copper foils to measure the potential difference. K-type thermocouples were used for measuring the hot and cold ends of the copper foil. One side of the sheet was exposed to the hot plate thus

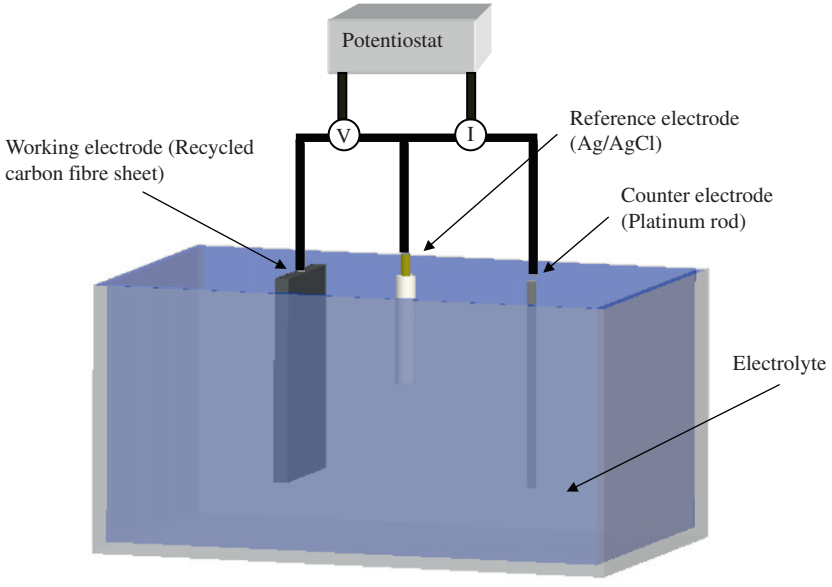

Fig. 1. Standard three cell electrode set up.

creating a hot side while the other side was exposed to room temperature. The gradient of $\Delta V/\Delta T$ is used in order to calculate the absolute Seebeck coefficient using Eq. (2). The measurements are repeated 5 times to get an average value. The test was conducted with an average measuring temperature of 40 °C. All potential and temperature readings were measured at the same point as indicated in [25]. Fig. 2 shows the experimental setup of the Seebeck coefficient test in the laboratory. The setup was similar to the methods in [9,26].

2.4. Electrical resistivity measurement

The electrical resistivity of the recycled carbon fibre sheets were measured using a Jandel Universal Probe with a RM3-AR test unit. The four point probe relies on measuring the voltage and current across the material with the probes equally spaced at 1 mm for this particular setup. Appropriate corrections were used according to the thickness to probe spacing ratio. Assuming infinite plane sample of finite thickness, the recycled carbon fibre sheets electrical resistivity was calculated. The thickness of the sheet was measured separately according to the ISO 534:2005 standard.

2.5. X-ray diffraction (XRD)

Phase and composition analysis were carried out with a PANalytical-X'Pert powder X-ray diffraction unit with a standard scintillation detector using CuKα radiation ($\lambda = 1.542$ A). The thermoelectric substrates were cut into a small sample size and then transformed into fine powder form using a standard mortar and pestle tool.

2.6. SEM and EDX analysis

The substrates were cut into small pieces and then mounted on a sticky carbon layer. The scanned electron images were taken using the JEOL 6400 microscope. Since the recycled carbon fibre sheets are conductive in nature, therefore no further sample preparation is needed. Energy dispersive X-ray was also conducted in order to determine the bismuth and tellurium composition on the substrate. The acceleration voltage of 10 kV was used for all the measurements.

3. Results and discussion

3.1. Cyclic voltammetry

The motivation behind using cyclic voltammetry analysis was to find the appropriate deposition potential range which will ultimately affect the depositing substrate's composition. The cyclic voltammetry graph in Fig. 3 shows the analysis using a bath concentration of 8 mM Bi^{3+} and 10 mM $HTeO^{2+}$. From Fig. 3, two distinctive reduction peaks can be clearly seen at 0.02 V and −0.06 V. The first peak corresponds to a reduction in tellurium while the second relates to a bismuth reduction.

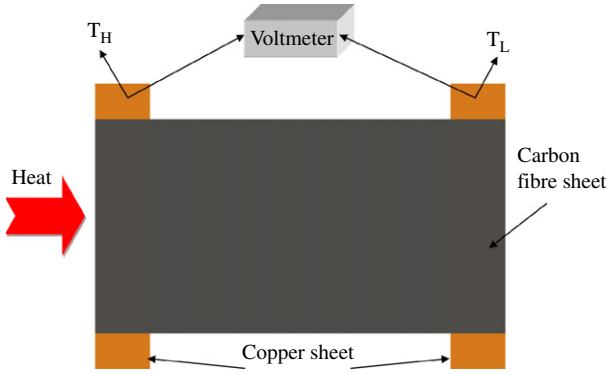

Fig. 2. Experimental setup for the Seebeck coefficient measurements.

The equation for the fundamental formation of bismuth telluride through electrodeposition is [27]

$$3HTeO_2^+ + 2Bi^{3+} + 9H^+ + 18e^- \rightarrow Bi_2Te_3 + 6H_2O \quad E^0 = 0.483 \text{ Vvs.NHE} \tag{3}$$

The main usage of the nitric acid is to complex the solution so that both the bismuth and tellurium ions would coexist at the same depositing potential [28]. The investigated deposition potential range for the formation of bismuth telluride was from −0.1 to −0.4 V.

3.2. Seebeck coefficient and electrical resistivity results

The Seebeck coefficient of the substrates which were electrodeposited at different potential based on the cyclic voltammetry analysis was shown in Fig. 4. An N-type material was formed using the specified bath concentration. From Fig. 4, the Seebeck coefficient values increase with a negative shift, while reaching the largest Seebeck coefficient of about $-54\ \mu V\ K^{-1}$ at −0.2 V. The Seebeck coefficient of the substrate would then decrease subsequently with a negative shift of potential. The N-type nature of the substrates depends largely on the chemical composition of the depositing films where it could be controlled using the right chemical molarity and depositing potential. Fig. 5 shows the effects of varying deposition potential on substrate's electrical resistivity. The electrical resistivity of the combined substrates on the other hand actually increases as the deposition potential reaches the optimum threshold from −0.1 V to −0.2 V. It however starts to decrease rapidly once the deposition potential increases past the deposition threshold. This is not surprising since the electron concentration is proportional to the material electrical conductivity while it varies inversely for the Seebeck coefficient. The lowest electrical resistivity value, $2.95 \times 10^{-5}\ \Omega$ m was obtained at the deposition potential of −0.131 V. The coating of bismuth telluride films onto to the recycled carbon fibre sheet managed to further decrease the sheet's electrical resistivity with its original resistivity at $4.6 \times 10^{-4}\ \Omega$ m. From both Figs. 4 and 5, the absolute value of the Seebeck coefficient increases from −0.1 to −0.2 V while the electrical resistivity did decrease slightly from −0.1 to −0.131, while the resistivity values increases from −0.131 onwards. Even though there was some decrease in electrical resistivity from −0.1 V to −0.131 V, it is only a small amount (8% difference), which might be attributed to the almost stoichiometric formation ($Bi_2Te_{2.8}$) of bismuth telluride.

Table 1 shows the properties of T-800s recycled carbon fibre sheets. With the combination of bismuth telluride compound, an increase of up to $47\ \mu V\ K^{-1}$ was observed while still preserving its N-type behaviour. This is expected as an addition of a higher Seebeck coefficient material (Bi_2Te_3) would result in an overall composite gain. The electrical conductivity of the total composite was also greatly increased with the presence of a much higher electrical conductivity material (Bi_2Te_3). This is also expected with the rule of mixture prevailing in this scenario. Overall, both the electrical conductivity and Seebeck coefficient managed to increase with the addition of bismuth telluride through electrodeposition.

3.2.1. Deposition potential effects on seebeck coefficient and electrical properties

The electrical conductivity and Seebeck coefficient fluctuates with the deposition potential due to the big differences in the

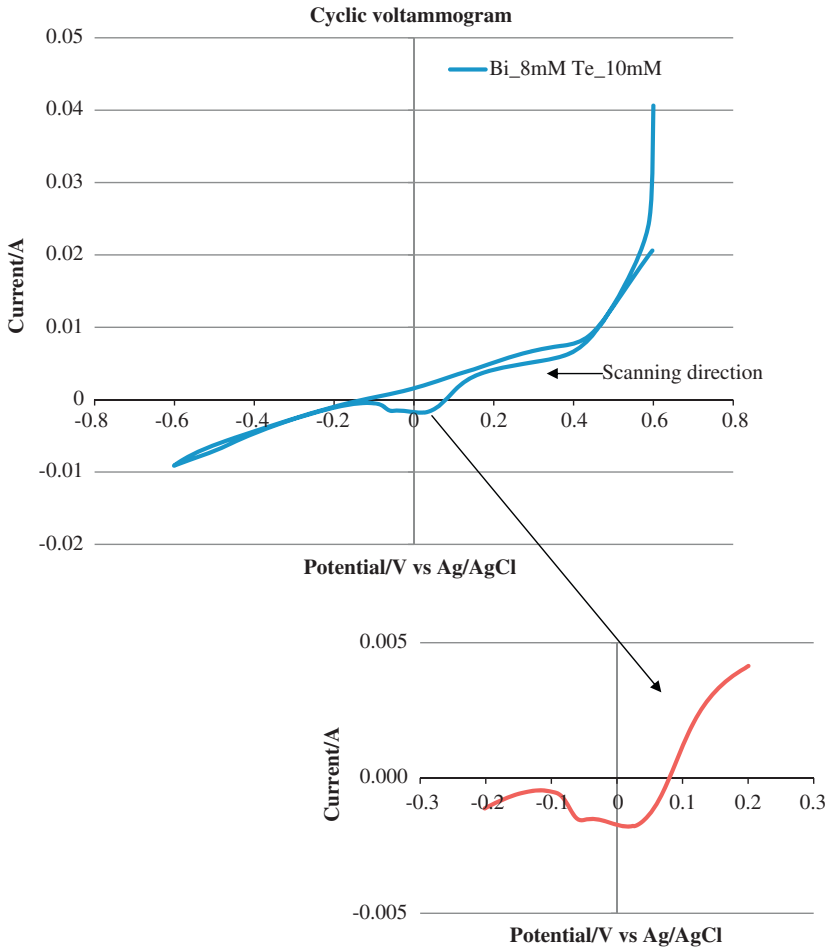

Fig. 3. Cyclic voltammogram with the recycled carbon fibre as a working electrode in a bath concentration of 8 mM Bi^{3+} and 10 mM $HTeO_2^+$ at a scanning rate of 10 mV/s.

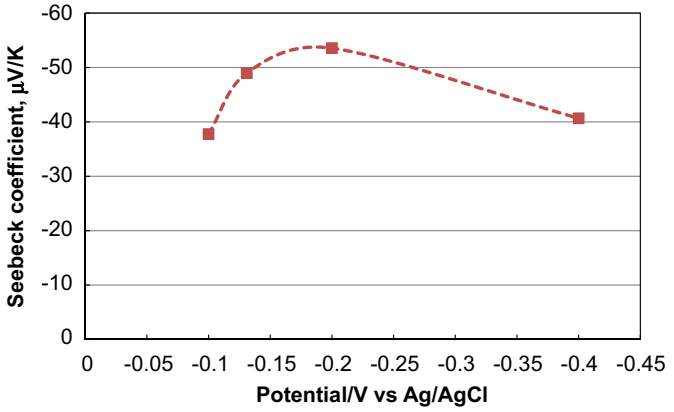

Fig. 4. Effects of varying deposition potential on the Bi_xTe_y coated recycled carbon fibre sheet's Seebeck coefficient at a bath concentration of 8 mM Bi^{3+} and 10 mM $HTeO_2^+$.

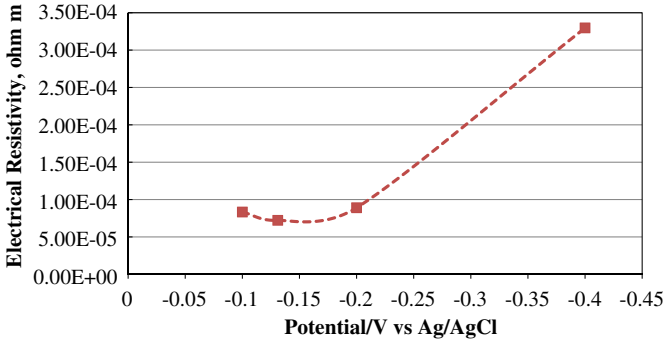

Fig. 5. Effects of varying deposition potential on the Bi_xTe_y coated recycled carbon fibre sheet's electrical conductivity at a bath concentration of 8 mM Bi^{3+} and 10 mM $HTeO_2^+$.

reduction of tellurium and bismuth. At each deposition potential, a combination of both bismuth and tellurium reduction determines the carrier concentration which subsequently determines the compound's electrical conductivity and Seebeck coefficient. As the depositing potential gets closer to Bi_2Te_3 reduction potential (Eq. (3)), It yields a more stochiometric compound hence producing better thermoelectric properties. This was demonstrated in Section 3.2.2 whereby the deposition potential of −0.131 V yields the closest stoichiometric compound and the highest power factor.

Table 1
Un-tampered T-800s recycled carbon fibre sheet properties.

T800s-Recycled carbon fibre sheet	
Seebeck coefficient	−6.16 μV/K
Electrical conductivity	4.33E−04 Ω m

3.2.2. *Power factor and Z_T*

Table 2 shows the power factor and Z_T of each composite and its respective depositing potential. The highest power factor and Z_T value were obtained through the compound deposited

at −0.131 V. This was due to its lower electrical resistivity values compared to other compounds and its moderate Seebeck coefficient value. This deposition potential value occurs just at the end of its reduction peak (Fig. 3), which allows both bismuth and tellurium enough potential to be reduced hence forming the right combination of Bi_2Te_3. Even though the Z_T value is low for commercial usage, it possesses good flexibility properties due to its carbon fibre core. Hence, this allows it to be used in sensors application where flexibility is needed.

3.3. XRD analysis

XRD analyses were conducted to determine the chemical structure of the deposited film. From Fig. 6, the XRD analysis of the film deposited at potential −0.131 V confirms the peak corresponds to the formation of stoichiometric Bi_2Te_3 on the recycled carbon fibre. The peaks observed at $2\Theta = 27.67$, 37.92 and 41.08 are indexed to be hexagonal crystal Bi_2Te_3 compound (JCPDS, 15-863) where peaks at $2\Theta = 27.67$ are most intense along the hkl (015) plane, while the rest shows slightly weaker peaks. Similar intensity peaks were also found at the deposition potential of −0.1 V, −0.2 V and −0.4 V in Fig. 6. A slight shift in the (0110) plane in Fig. 6(b) was observed in comparison with Fig. 6(a); this could be attributed to the increase in tellurium content. Comparable findings were also observed in [29,30]

Table 2
Power factor and Z_T of each composite and its respective depositing potential.

Depositing Potential (V)	Electrical resistivity (Ω m)	Seebeck Coefficient (μV/k)	Power factor (W/m K^2)	Z_T*
−0.1	8.33E−05	−37.76	1.71E−05	5.13E−04
−0.131	7.22E−05	−48.96	3.32E−05	9.96E−04
−0.2	8.91E−05	−53.56	3.22E−05	9.66E−04
−0.4	3.30E−04	−40.66	5.01E−06	1.50E−04

* Z_T values calculated assuming carbon fibre's thermal conductivity value.

3.4. SEM analysis and EDX

Fig. 7 shows the effects of various deposition potentials on the fibre's surface morphology. At a lower deposition potential −0.1 V, a somewhat rough crystal like structure can be observed with a lower bismuth content compared to the conventional 60% Te and 40% Bi as shown in Table 3. This could be attributed to the low deposition voltage causing more reduction of bismuth ions compare to tellurium ions. EDX analysis shows that the composition of film prepared at −0.131 V is $Bi_2Te_{2.8}$ (Table 3), which is the closest composition to the perfect composition of Bi_2Te_3. The surface morphology of the Bismuth Telluride deposited at −0.1 and −0.2 V looks rather similar with rough and uniform surfaces while at −0.131 V, strand-like surfaces can be seen clearly. Rough, loose and dendritic growth could be seen for films deposited at a higher deposition potential of −0.4 V. The tellurium content tends to increase nearer to 60% as the deposition potential increases from −0.1 to −0.131 V, while it starts to decline as it approaches −0.4 V. Hence it can be concluded that the perfect range of obtaining an optimal chemical composition of Bi_2Te_3 compound lies between −0.131 V to −0.2 V.

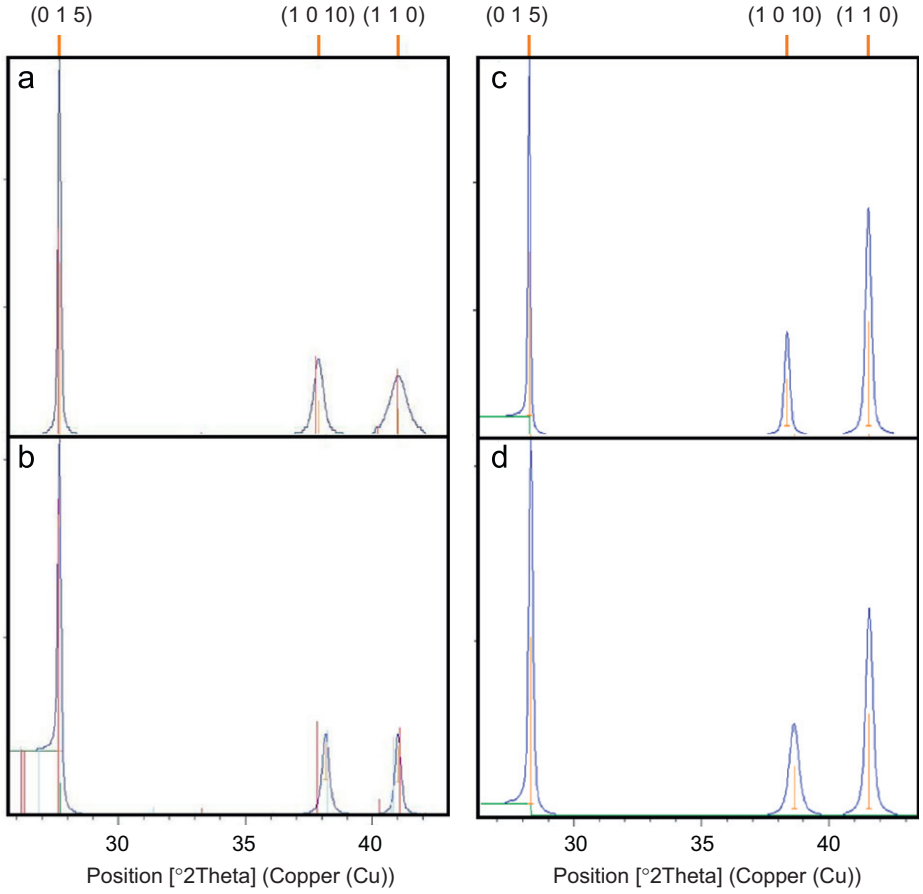

Fig. 6. XRD pattern for Bi_xTe_y substrate electrodeposited at (a) −0.1 V, (b) −0.131 V, (c) −0.2 V and (d) −0.4 V.

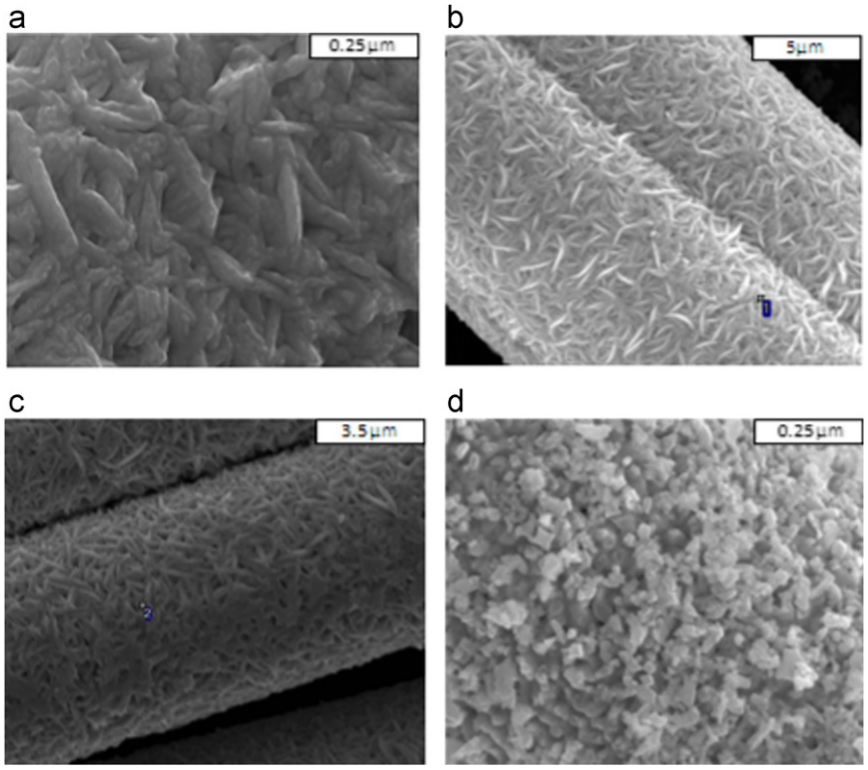

Fig. 7. SEM images of the various Bismuth telluride deposited recycled carbon fibres at deposition potential (a) −0.1 V, (b) −0.131 V, (c) −0.2 V and (d) −0.4 V.

Table 3
Effects of varying electrodeposition potential on the compositions of the Bi_xTe_y films deposited in a nitric acid solution.

E/V (vs. Ag/AgCl)	Bi	Te	Formula
	(at %)		
−0.1	43.36	56.64	$Bi_2Te_{2.6}$
−0.131	41.6	58.4	$Bi_2Te_{2.8}$
−0.2	41.9	58.1	$Bi_2Te_{2.77}$
−0.4	47.16	52.84	$Bi_2Te_{2.24}$

3.4.1. Composition analysis

As the deposition potential increases in the negative direction, the bismuth content starts to increase. This is because as the potential increases towards the negative direction, the tellurium reduction peak gets further away hence this increases the formation of bismuth content; while the compound deposited at −0.1 V, according to Martin [31] the Bi^{3+} reduction potential is just slightly more negative than the reduction of Bi_2Te_3 (Eq. (3)). Hence these result in a higher increase of bismuth deposition at a lower deposition potential.

The electrical conductivity and Seebeck coefficient fluctuates with the deposition potential due to the big differences in the reduction of tellurium and bismuth. At each deposition potential, a combination of both bismuth and tellurium reduction determines the carrier concentration which subsequently determines the compound's electrical conductivity and Seebeck coefficient. As the depositing potential get closer to Bi_2Te_3 reduction potential (Eq. (3)), it yields a stoichiometric compound and produce better thermoelectric properties. This was demonstrated in Section 3.2.2, where the deposition potential of −0.131 V yields the closest stoichiometric compound and the highest power factor. Even though all of the deposits are bismuth rich (Bi > 40%), the measured Seebeck coefficient showed an N-type behaviour. Similar findings were also found in other papers [16,29,32,33]. This could be explained through [32] whereby it was reported that the existence of a tellurium rich layer close to the substrate forms a P–N junction with the Bi-rich (p-type) deposit. With the N-type layer having a large excess of donors while the p-type layer having a small acceptor count, the Fermi level of the P–N junction moves towards the negative potential direction as temperature rises. Hence the resultant P–N layers caused a negative Seebeck measurement even though the Hall effect measurement indicates a P-type behaviour.

4. Conclusion

Bismuth telluride films were successfully synthesised on recycled carbon fibre using potentiostatic electrodeposition. The films had a range 53–58 at% deposited tellurium which was controlled by the deposition potential while all the films exhibit an N-type semiconductor characteristic. The surface morphology of tellurium rich Bi_xTe_y films were strand-like crystal structure while bismuth rich Bi_xTe_y films have rough and uniform surfaces. XRD analysis confirmed the formation of Bi_2Te_3 compound with a high intense peak along the (015) crystal plane. Cyclic voltammetry analysis shows the reduction of both bismuth and tellurium occurs within −0.11 V–0.075 V range. The Seebeck coefficient of the bismuth telluride recycled carbon fibre sheet reached a maximum ($-54\ \mu V\ K^{-1}$) at the near stoichiometric composition of Bi_2Te_3, deposited at −0.2 V.

Acknowledgments

This research is sponsored by Nottingham Innovative Manufacturing Research Centre (NIMRC), Engineering and Physical Sciences Research Council (EPSRC), the Cradle Fund and Cheesun Technology Company. The author would also like to thank our

industrial partners: Technical Fibre Products and Boeing for their contributions.

References

[1] S.J. Pickering, R.M. Kelly, J.R. Kennerley, C.D. Rudd, N.J. Fenwick, Compos. Sci. Technol. 60 (4) (2000) 509–523.
[2] S.J. Pickering, Compos. A Appl. Sci. Manuf. 37 (8) (2006) 1206–1215.
[3] V.P. McConnell, Reinf. Plast. (2010).
[4] J.R. Hyde, E. Lester, S. Kingman, S. Pickering, K.H. Wong, Compos. A Appl. Sci. Manuf. 37 (11) (2006) 2171–2175.
[5] G. Jiang, S.J. Pickering, E.H. Lester, T.A. Turner, K.H. Wong, Compos. Sci. Technol. 69 (2) (2009) 192–198.
[6] KH Wong, SJ Pickering, CD. Rudd, Compos. A Appl. Sci. Manuf. 41 (2010) 6.
[7] I.V. Klimenko, T.S. Zhuravleva, V.M. Geskin, T. Jawhary, Mater. Chem. Phys. 56 (1) (1998) 14–20.
[8] Y.S. Lee, B.K. Lee, Carbon 40 (13) (2002) 2461–2468.
[9] S. Wang, D.D.L. Chung, Compos. Interface. 6 (6) (1999) 12.
[10] C. Silva, E. Marotta, M. Schuller, L. Peeml, M. O'Neill, Anglais 21 (3) (2007) 8.
[11] E.J.X. Pang, A. Chan, S.J. Pickering, Compos. A Appl. Sci. Manuf. 42 (10) (2011) 1406–1411.
[12] H. Böttner JN, A. Gavriko, G. Kühner, M. Jägle, C. Kunzel, D. Eberhard, G. Plescher, A. Schbert, K.H. Schlereth, J. Microelecton. Syst. 13 (2004).
[13] R. Venkatasubramanian, E. Siivola, T. Colpitts, B. O'Quinn, Nature 413 (6856) (2001) 597–602.
[14] H. Zou, D.M. Rowe, G. Min, J. Cryst. Growth. 222 (1-2) (2001) 82–87.
[15] H. Zou, D.M. Rowe, G. Min, J. Vac. Sci. Technol. A 19 (3) (2001) 899–903.
[16] B.Y. Yoo, C.K. Huang, J.R. Lim, J. Herman, M.A. Ryan, J.P. Fleurial, et al., Electrochim. Acta 50 (22) (2005) 4371–4377.
[17] L., Qiu J. Zhou, X. Cheng, R. Ahuja, Electrochemical deposition of Bi2Te3-based thin films, Journal of Physics and Chemistry of Solids, 71(8) pp. 1131–1136.
[18] F. Li, W. Wang, Appl. Surf. Sci. 255 (7) (2009) 4225–4231.
[19] S.-G. Kang, T. Kobayashi, Mater. Sci. Forum 377 (2004) 449–452.
[20] C. Boulanger, J. Electron. Mater. 39 (9) (2010) 1818–1827.
[21] D. Pinisetty, D. Davis, E.J. Podlaha-Murphy, M.C. Murphy, A.B. Karki, D.P. Young, et al., Acta Mater. 59 (6) (2011) 2455–2461.
[22] Toray Carbon fibers America I, Torayca T800s data sheet, Technical data sheet No CFA-019: Toray Inc. America, 2011.
[23] M.T. Tritt, in: D.M. Rowe (Ed.), Thermoelectrics Handbook: Macro to Nano:, CRC Talyor and Francis, 2006, p. 23-1-0.
[24] S. Wen, D.D.L. Chung, Cem. Concr. Res. 34 (12) (2004) 2341–2342.
[25] J. Martin, T. Tritt, C. Uher, J. Appl. Phys. 108 (12) (2010) 12.
[26] S. Wen, D.D.L. Chung, Cem. Concr. Res. 30 (8) (2000) 1295–1298.
[27] P. Magri, C. Boulanger, J.-M. Lecuire, J. Mater. Chem. 6 (5) (1996) 773–779.
[28] Y. Ma, E. Ahlberg, Y. Sun, B.B. Iversen, A.E.C. Palmqvist, Electrochim. Acta 56 (11) (2011) 4216–4223.
[29] M.-Y. Kim, T-S. Oh, J. Electron. Mater. 38 (7) (2009) 1176–1181.
[30] Y. Ma, A. Johansson, E. Ahlberg, A.E.C. Palmqvist, Electrochim. Acta 55 (15) (2010) 4610–4617.
[31] M.S. Martin-Gonzalez, A.L. Prieto, R. Gronsky, T. Sands, A.M. Stacy, J. Electrochem. Soc. 149 (11) (2002) 546–554.
[32] Makoto Takahashi, Masashi Kojima, Shoji Sato, Naoyuki Ohnisi, Akira Nishiwaki, Koichi Wakita, et al., J. Appl. Phys. 96 (10) (2004) 6.
[33] Y. Miyazaki, T. Kajitani, J. Cryst. Growth. 229 (1–4) (2001) 542–546.